Eur. Phys. J. A **29**, 271–280 (2006)
DOI 10.1140/epja/i2006-10088-6

THE EUROPEAN PHYSICAL JOURNAL A

Mass measurements of neutron-deficient nuclides close to A = 80 with a Penning trap

A. Kankainen[1,a], L. Batist[2], S.A. Eliseev[2,3], V.-V. Elomaa[1], T. Eronen[1], U. Hager[1], J. Hakala[1], A. Jokinen[1], I. Moore[1], Yu.N. Novikov[2], H. Penttilä[1], K. Peräjärvi[1], A.V. Popov[2], S. Rahaman[1], S. Rinta-Antila[1], P. Ronkanen[1], A. Saastamoinen[1], D.M. Seliverstov[2], T. Sonoda[1], G.K. Vorobjev[2,3], and J. Äystö[1]

[1] Department of Physics, P.O. Box 35, FI-40014 University of Jyväskylä, Finland
[2] Petersburg Nuclear Physics Institute, 188300 Gatchina, Russia
[3] GSI, Postfach 110552, D-64291 Darmstadt, Germany

Received: 28 April 2006 / Revised: 3 July 2006 /
Published online: 14 September 2006 –
Communicated by D. Guerreau

Abstract. The masses of ^{80,81,82,83}Y, ^{83,84,85,86,88}Zr and ^{85,86,87,88}Nb have been measured with a typical precision of 7 keV by using the Penning trap setup at IGISOL. The mass of ^{84}Zr has been measured for the first time. These precise mass measurements have improved S_p and Q_{EC} values for astrophysically important nuclides.

PACS. 21.10.Dr Binding energies and masses – 27.50.+e $59 \leq A \leq 89$

1 Introduction

The masses of neutron-deficient nuclides close to $A = 80$ are important for modeling the astrophysical rapid proton capture process (rp process) [1]. The rp process occurs as a sequence of proton captures and β^+ decays in various astrophysical sites, such as on the surface of an accreting neutron star (see, *e.g.*, ref. [2]). The flow of the rp process follows a path close to the $N = Z$ nuclei up to ^{56}Ni. At higher masses, the path broadens and shifts by about one or two units towards stable nuclei. The path is wider for steady-state burning (*e.g.*, in X-ray pulsars) than for X-ray bursts. It is shown for relevant nuclei in steady-state burning conditions in fig. 1. Regardless of the burning type, the rp process can proceed up to $A \approx 100$ ending in a closed SnSbTe cycle [3]. Earlier it was proposed that the rp process would end in a Zr-Nb cycle in which ^{83}Nb is processed back to ^{80}Zr via (p, α) reactions [2]. However, the existence of the Zr-Nb cycle depends on the α separation energy of ^{84}Mo which has not been measured.

The rp process is mainly determined by nuclear masses and β^+ decay half-lives of the nuclides on its path [2]. The theoretical mass predictions for the nuclides in the $A = 80$ region give too high uncertainties for the rp process calculations and therefore, reliable experimental data on masses are needed. The rp process models depend critically on the Q values for proton captures which drive the path towards the proton drip line until a waiting-point nucleus is reached. In order to estimate the proton capture rates, the masses and excitation energies should be known better than 10 keV [4].

At a waiting point, an equilibrium between proton captures and photodisintegration is established and the rp process can continue only via a 2p capture or a β^+ decay. As the destruction rate of a waiting-point nucleus depends exponentially on its one-proton capture or two-proton capture Q values [2], nuclear masses play the main role close to the waiting-point nuclides, such as ^{80}Zr in the $A \approx 80$ region. In this mass region, the rapid changes in nuclear structure make the extrapolation of masses and prediction of half-lives very difficult. As the half-life predictions depend severely on the Q_{EC} values due to the energy dependence of the Fermi function, the Q_{EC} values for β^+ decays with unknown half-lives are of special interest. In general, actual beta-decay schemes and therefore Q_{EC} values, have to be known in order to determine the energy production of the rp process [4]. In this paper, we present new mass measurement data on 13 neutron-deficient isotopes of Y, Zr and Nb approaching the $Z = N$ line.

Isomeric states are common for nuclides close to $A = 80$. Previously, these isomers have been studied spectroscopically (see refs. [5,6]) using the HIGISOL technique (Heavy-ion Ion Guide Isotope Separator On-Line [7]). Nevertheless, excitation energies of many isomers in this region are still unknown, such as ^{85}Nb^m and ^{86}Nb^m. The identification of these isomeric states would be an impor-

[a] e-mail: anu.kankainen@phys.jyu.fi

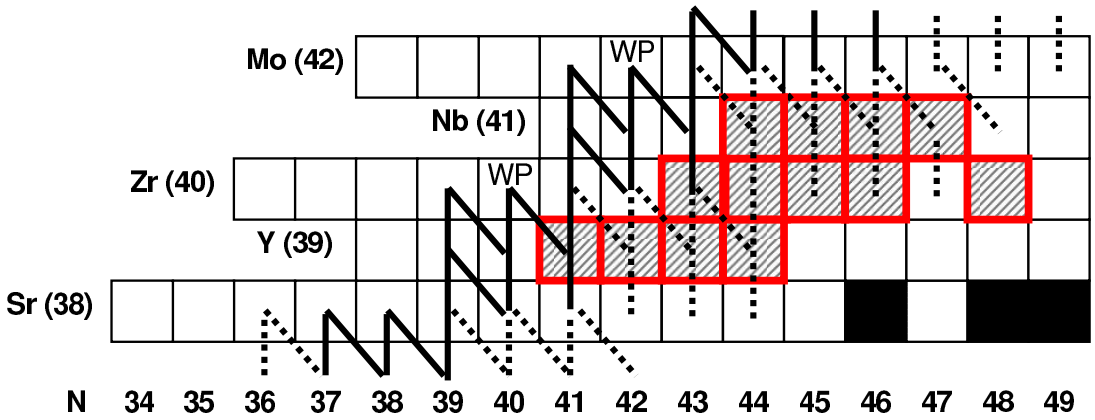

Fig. 1. The rp process path in the region close to $A = 80$ for steady-state burning [3]. The reaction flows of more than 10% are shown by a solid line and of 1–10% by a dotted line. The studied nuclides are highlighted by squares. Waiting-point nuclei ^{80}Zr and ^{84}Mo are labeled as WP.

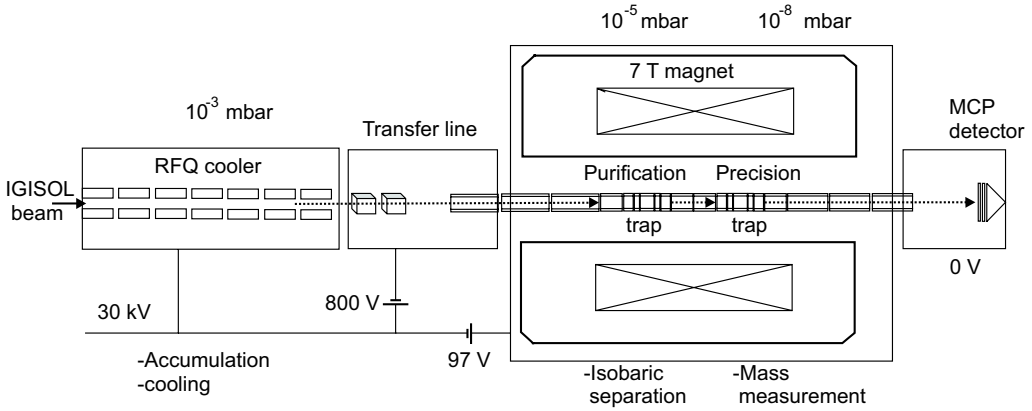

Fig. 2. A schematic figure of the JYFLTRAP setup.

tant input to nuclear-reaction network calculations modeling the rp process.

2 Experimental method

The isotopes of interest were produced by a ^{32}S beam from the Jyväskylä K-130 cyclotron impinging on an enriched ^{54}Fe or ^{nat}Ni target. The reaction products were stopped in the HIGISOL gas cell at the IGISOL facility [8]. After the extraction from the gas cell by a helium flow and a small extraction potential, the ions were accelerated to 30 keV and mass-separated by a 55° dipole magnet ($M/\Delta M \approx 500$). The yields were about the same as in a previous experiment [6] which focused on the spectroscopy of the isomeric states in this mass region.

Mass-separated ions of interest were sent to the radiofrequency quadrupole ion beam cooler and buncher [9]. After cooling and accumulating for a short time the ions were extracted as a short bunch and transported to the Penning trap system. The JYFLTRAP setup is shown in fig. 2. It consists of two cylindrical Penning traps in a superconducting magnet with a field strength of 7 Tesla [10]. The traps are placed in the homogeneous regions of the magnet separated by 20 cm. The first trap, the purification trap filled with helium gas at a pressure of about 10^{-4} mbar, is dedicated for isobaric cleaning using a mass selective buffer gas cooling technique. The second trap called the precision trap operates in vacuum and is used for high-precision mass measurements employing the time-of-flight ion cyclotron resonance technique [11]. In a Penning trap ions possess three different eigenmotions: one axial and two radial motions, the latter corresponding to magnetron (ν_-) and reduced cyclotron motion (ν_+) with frequencies summing up to the true cyclotron frequency $\nu_c = \nu_- + \nu_+$.

Cooled and bunched ions from the buncher captured in the purification Penning trap were further cooled axially by collisions with helium atoms and stored at the center of the trap. Possible isobaric contaminations were removed by the application of RF dipole excitations in combination with helium buffer gas. Immediately after that a RF quadrupole excitation at a mass-dependent cyclotron frequency (ν_c) was applied which leads to centering of the ions of interest. A total cycle time of about 400 ms was used and a mass resolving power of about 10^5 could be reached in this configuration. The cleaning procedure has been described in detail in ref. [12].

Isobarically purified and cooled ions were transported to the precision trap. In this trap, RF dipole excitations

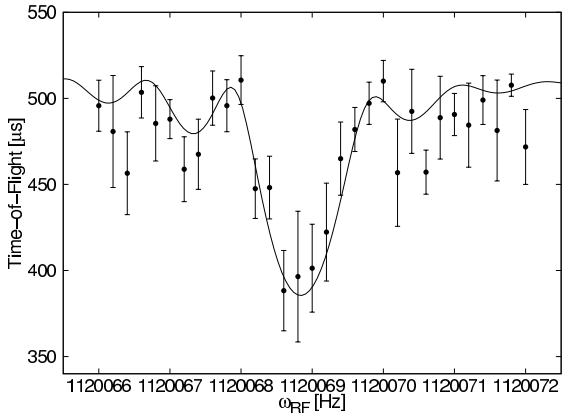

Fig. 3. Time-of-flight resonance of ^{80}Y with an excitation time of 900 ms. The fit of the experimental data points is shown by a solid line.

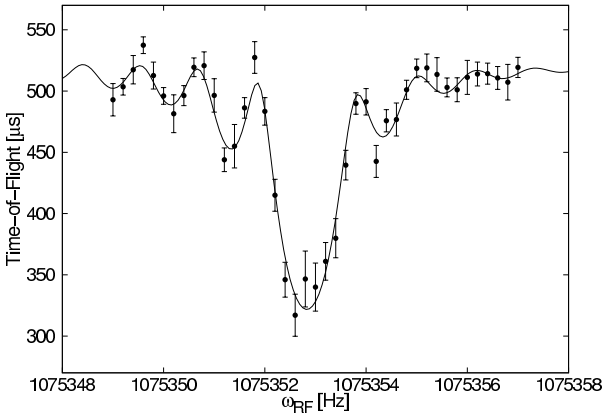

Fig. 4. Time-of-flight resonance of ^{84}Zr with an excitation time of 900 ms. The fit of the experimental data points is shown by a solid line.

employing the phase-locking technique [13] were applied in order to enhance the magnetron radius. Then the RF quadrupole excitations were applied to convert periodically a slow magnetron motion to a fast reduced cyclotron motion with a higher radial energy. An excitation time of 900 ms was chosen with a corresponding excitation amplitude which finally allows a full conversion to the reduced cyclotron motion at the resonance frequency. Finally, the ions were ejected from the trap. They drift towards the micro channel plate (MCP) detector through a set of drift tubes where a strong magnetic-field gradient exists. Here the ions experience an axial force which converts the radial kinetic energy of the ions into longitudinal energy. As a result, an ion in-resonance with the applied quadrupole excitation field moves faster towards the detector than an ion which was off-resonance. By measuring the time of flight as a function of the applied excitation frequency, the cyclotron frequency of the ions under investigation was determined. The mass of an ion can be determined:

$$\nu_c = \frac{q}{2\pi m} B, \qquad (1)$$

where ν_c is the cyclotron frequency of the ion, m is the mass and q is the charge state of the ion. The magnetic

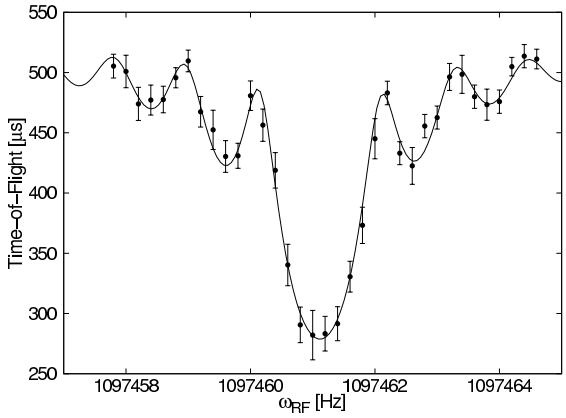

Fig. 5. Time-of-flight resonance of a reference nucleus ^{98}Mo with an excitation time of 900 ms. The fit of the experimental data points is shown by a solid line.

field B is calibrated with a well-known reference mass. Stable Mo isotopes ^{96}Mo and ^{98}Mo originating from the Havar window of the HIGISOL facility were used as references in this experiment. Examples of the measured time-of-flight resonances are shown for the odd-odd nucleus ^{80}Y (fig. 3), for the even-even nucleus ^{84}Zr (fig. 4) and for a reference nucleus ^{98}Mo (fig. 5).

In summary, overall precision of 7×10^{-8} was achieved in these measurements. Typical transmission from the focal plane of IGISOL through the cooler and trap system was about one percent.

3 Results

The masses of $^{80-83}$Y, $^{83-86,88}$Zr and $^{85-88}$Nb were measured during this experiment. All measurements were done with 900 ms excitation time in the precision trap. The stable isotopes $^{96-98}$Mo were used as reference masses. In order to test the reliability of the system, ^{96}Mo and ^{98}Mo were measured relative to ^{97}Mo. As shown in table 1, the results for the Mo isotopes agree nicely with the values of the 2003 Atomic Mass Evaluation (AME) [14]. Except for the stable Mo references, all nuclides were measured as oxides formed with ^{16}O in the HIGISOL.

The results of the analysis are given in table 1. Apart from the uncertainty of the reference masses, 1.9 keV for ^{96,97,98}Mo, and in the case of oxides that of ^{16}O (0.0001 keV), three systematic uncertainties were taken into account in the analysis.

Firstly, in an offline study comparing ^{129}Xe to $^{16}O_2$ the resonance frequency was found not to be perfectly linear in mass, but to have a slight offset of 7×10^{-10} per mass unit difference between the compared masses. This shift was accounted for by quadratically adding this uncertainty multiplied by the difference in mass number between the reference and the measured nucleus (molecule for the oxides) to the uncertainty of the final average for each studied nucleus.

Secondly, large numbers of ions in the trap can cause the frequency to shift. In this experiment, typically about

Table 1. Overview of the measured mass excesses (ME) compared to the tabulated values [14]. The reference nuclides and number of measurements (N) are given for the measured isotopes. All masses are for the ground states (see sect. 4.1). The mass excesses are based on the frequency ratio of the reference nucleus to the measured nucleus (ν_{ref}/ν) given in the table. The error for the difference AME-JYFL is dominated by the uncertainties in the AME mass excesses.

Nuclide	Reference	N	ν_{ref}/ν	ME(JYFL) (keV)	ME(AME) (keV)	AME-JYFL (keV)
^{80}Y	^{96}Mo	3	1.00025645(7)	−61144(7)	−61220(180)	−76(180)
^{81}Y	^{97}Mo	3	1.00018938(6)	−65709(6)	−66020(60)	−311(60)
^{82}Y	^{98}Mo	7	1.00016793(6)	−68060(6)	−68190(100)	−130(100)
^{83}Y†	^{98}Mo	3	1.01033685(6)	−72170(6)	−72330(40)	−160(40)
^{83}Zr	^{98}Mo	2	1.01040553(7)	−65908(7)	−66460(100)	−552(100)
^{84}Zr	^{98}Mo	4	1.02055911(6)	−71418(6)	−71490(200)	−72(200)
^{85}Zr	^{98}Mo	3	1.03075388(7)	−73170(6)	−73150(100)	20(100)
^{86}Zr	^{98}Mo	3	1.04091538(7)	−77958(7)	−77800(30)	158(30)
^{88}Zr	^{98}Mo	3	1.06128125(7)	−83624(7)	−83623(10)	1(12)
^{85}Nb†	^{98}Mo	3	1.03082952(7)	−66273(7)	−67150(220)	−877(220)
^{86}Nb	^{98}Mo	5	1.04101219(6)	−69129(6)	−69830(90)	−701(90)
^{87}Nb†	^{98}Mo	2	1.05117423(7)	−73868(7)	−74180(60)	−312(60)
^{88}Nb†	^{98}Mo	3	1.06136322(7)	−76149(7)	−76070(100)	79(100)
^{96}Mo	^{97}Mo	3	0.98966683(6)	−88789(6)	−88790.5(19)	−2(6)
^{98}Mo	^{97}Mo	3	1.01031302(6)	−88111(6)	−88111.7(19)	−1(6)

† Possible contributions from ^{83}Y^m at 61.98(11) keV, ^{85}Nb^m at $\geq$ 69 keV, ^{87}Nb^m at 3.84(14) keV and ^{88}Nb^m at 40(140) keV have not been taken into account. For a possible treatment of mixtures of isomeric and ground states, see ref. [15] pp. 174–180.

500–1000 ions were used for the analysis after setting time and countrate windows. To estimate the resulting uncertainty, an analysis of the frequency depending on the countrate was done for all measurements of ^{98}Mo. A shift of about 0.01 Hz per ion, mostly towards higher frequencies, was observed. Since ^{98}Mo is stable, only a few impurities are expected to be in the trap, and the effect is expected to be smaller than for unstable nuclei, where impurities are produced by decay. However, since all nuclides studied in this work have half-lives considerably longer than the employed excitation time, this difference is small. In the final analysis the maximum number of ions in the trap was therefore limited to three, and an uncertainty of 0.04 Hz was quadratically added to the uncertainty of the final average for each nucleus, corresponding to about 3 keV in this mass range.

Thirdly, to compensate for fluctuations of the magnetic field and of the electronics, the fluctuation of the measured frequency of ^{98}Mo from one measurement to the next was examined. The average instability was found to be of the order of 0.04 Hz. Since the fluctuation is assumed to be completely random, this value was quadratically added to the statistical uncertainty of each measured frequency; its influence decreases with an increasing number of measurements for the nucleus.

4 Discussion

In this section, the role of isomeric states in the measured nuclides is discussed. The results for Y, Zr and Nb isotopes are reported nuclide by nuclide and compared to earlier experiments and the values of the 2003 Atomic Mass Evaluation. Proton separation energies and Q_{EC} values determined for the measured nuclides are collected in tables 3 and 4.

4.1 Isomers

Several of the measured nuclides have isomeric states (see table 2). The observation of these isomers is experimentally limited by the half-life, the excitation energy and by

Table 2. Isomeric states as listed in the NUBASE compilation [16]. Given are the excitation energies, the half-lives and the spins and parities (J^π) for the isomeric and ground states.

Isomer	E_{exc} (keV)	$T_{1/2}$	J^π	$J^\pi_{g.s.}$
^{80}Y^m	228.5(1)	4.8 s	1^-	4^-
^{80}Y^n	312.5(10)	4.7 μs	(2^+)	4^-
^{82}Y^m	402.63(14)	268 ns	4^-	1^+
^{83}Y^m	61.98(11)	2.85 min	$3/2^-$	$9/2^+$
^{83}Zr^m	52.72(5)	530 ns	$(5/2^-)$	$(1/2^-)$
^{85}Zr^m	292.2(3)	10.9 s	$(1/2^-)$	$7/2^+$
^{85}Nb^{m†}	$\geq$ 69	3.3 s	$(1/2^-)$	$(9/2^+)$
^{86}Nb^m	250#(160#)	56 s	–	(6^+)
^{87}Nb^m	3.84(14)	2.6 min	$(9/2^+)$	$(1/2^-)$
^{88}Nb^m	40(140)	7.8 min	(4^-)	(8^+)

† The energy and half-life of ^{85}Nb^m are from ref. [6]. The appearance of a 759.0(10) keV isomer with $T_{1/2}$ = 12 s in ref. [16] is based on a misinterpretation of the result of ref. [32] where a β-coincident γ-ray with an energy of 759 keV was reported.

their relative production rate (isomer ratio). With typical production rates in this experiment, isomers with a half-life of less than 500 ms could not be measured due to the excitation time of 900 ms in the precision trap and a total cycle time of ~ 1.5 s. The FWHM of the time-of-flight resonance was about 1.2 Hz, or about 100 keV in this mass region. Thus, isomers with low excitation energies could not be resolved, again depending on the relative production rates.

Due to half-life and excitation energy limitations, only the isomeric states of ^{80}Y, ^{85}Zr, ^{85}Nb, and possibly ^{86}Nb and ^{88}Nb, are interesting for further studies. Larger frequency ranges were scanned to find a second resonance. For ^{80}Y^m, ^{85}Zr^m and ^{85}Nb^m the excitation energies are known, but no second resonance could be found at the corresponding distance from the measured resonance frequency. For ^{86}Nb, no second resonance was observed within about 450 keV and for ^{88}Nb the limit was about 310 keV.

Since in all of these cases only one state was observed, it is not possible to determine "*a priori*" whether the measured nucleus was the ground state or the excited state. In the case of ^{85}Nb, the measured mass would agree better with the tabulated value of the excited state than with the ground state (see ref. [16]). This is also the case for the other Nb isotopes. For Y and Zr isotopes, however, the measured mass is closer to the ground state. As only primary ions are mass-separated at IGISOL, the observed yields represent the isomeric and ground states as well. In general, heavy-ion reactions tend to favor the population of higher-spin states. Therefore, they favorably populate ground states in all studied cases except for ^{87}Nb where the energy is very small anyway (see table 2). For example, the isomers ^{80}Y^m, ^{85}Zr^m and ^{85}Nb^m are less produced than the ground states at HIGISOL. The isomeric to ground state ratios for these isotopes at HIGISOL are about 1 : 4 for ^{80}Y [5,17], 1 : 40 for ^{85}Zr [6] and 1 : 2 for ^{85}Nb [6].

4.2 Y isotopes

The results of the Y isotopes are presented in fig. 6 in comparison with the earlier results and the AME values. Most of the masses are based on measurements of end-point energies of β^+ spectra. The corresponding mass excesses have been calculated from the Q_{EC} values with the tabulated mass excesses of the daughter nuclides (^{80,81,82,83}Sr) [14]. Our measured mass excesses agree with the AME value only for the isotope ^{80}Y for which a time-of-flight measurement by use of a cyclotron has been performed.

4.2.1 ^{80}Y

Partly due to astrophysical motivation, the mass of ^{80}Y has been measured several times. The early beta-decay experiments yielded Q_{EC} values of 6952(152) keV [18], 6934(242) keV [19] and 6200(600) keV [20]. Although these values were consistent, the calculated mass excesses were more than 2 MeV too low compared to the AME value based on the systematics of neighboring isotopic and isotonic chains. A direct mass measurement of ^{80}Y using the second cyclotron of SARA of the ISN as a time-of-flight spectrometer gave a Q_{EC} value of 9120(170) keV [21] which proved that the earlier Q_{EC} values were too low. Due to this discrepancy, the results from [18,19] and [20] have been left out from fig. 6. The Q_{EC} value has also been recently measured via beta-gamma coincidence spectroscopy and a lower limit for the Q_{EC} value was measured to be 8929(83) keV [22] which corresponds a mass excess larger than $-61379(84)$ keV. The disagreement with the earlier β^+ end-point measurements is suggested to arise from the assumptions about β^+ feeding in the ^{80}Y decay scheme. The β^+ spectrum was earlier measured in coincidence with the two lowest-lying γ transitions from the levels at 386 keV and 981 keV [18,19] but in [22], the gating γ transition was from the highest fed level observed at 3284 keV. Thus, the β^+ decay of ^{80}Y should primarily feed a level or a set of levels above ≈ 3 MeV and not the low-lying levels.

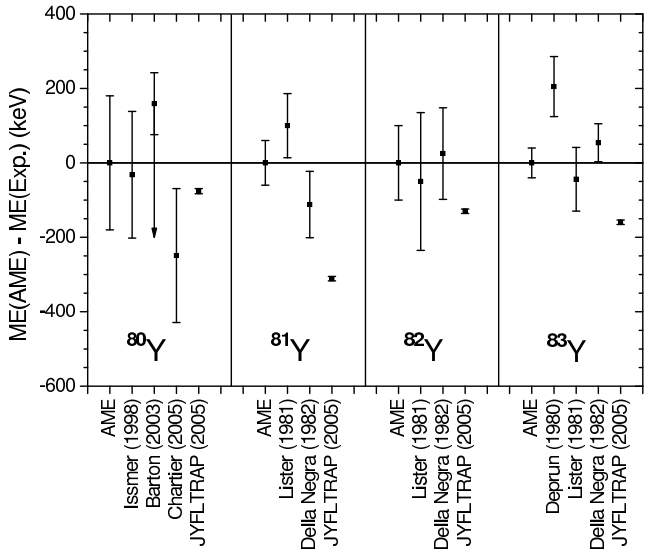

Fig. 6. Mass excesses of the measured Y isotopes relative to AME values [14]. The error bars represent only the uncertainties of the corresponding experiments. The labels refer to beta-decay experiments of Barton *et al.* [22], Lister *et al.* [18], Della Negra *et al.* [19], Deprun *et al.* [25] and to the TOF experiments at SARA by Issmer *et al.* [21] and at CSS2 by Chartier *et al.* [24]. The Q_{EC} value of ^{80}Y in [22] is only a lower limit which is indicated by an arrow in the figure.

There have also been two time-of-flight measurements using the second cyclotron of GANIL, CSS2, as a mass spectrometer of high resolution [23,24]. Due to a number of experimental difficulties in [23], the measured mass excess of $-62097(80)$ keV differs from the other existing experiments and is not included in fig. 6. The mass was re-measured at CSS2 resulting in a new mass excess of $-60971(180)$ keV [24] which agrees well with the values of $-61188(171)$ keV [21], the adopted AME value of

−61220(180) keV and −61144(7) keV from this work. Our measured mass corresponds to the ground state as the well-known isomer at 228.5 keV in ^{80}Y is much less produced than the ground state and no second resonance was found in a wider frequency range (see sect. 4.1). The other isomeric state at 312.5 keV in ^{80}Y (4.7 μs) was too short-lived for JYFLTRAP.

4.2.2 ^{81}Y

Our measured mass excess of −65709(6) keV does not agree with the AME value which is based on beta-decay experiments of refs. [18] and [19]. In ref. [18], a Q_{EC} value of 5408(86) keV was determined from coincidences with 124 keV and 408 keV γ-rays in ^{81}Sr and the deduced mass excess is −66120(87) keV. In ref. [19], the mass and the 124 keV γ transition measured with a plastic scintillator were used to gate the β^+ spectrum, which resulted in a Q_{EC} value of 5620(89) keV and a mass excess of −65908(90) keV. Although the adopted Q_{EC} value of [19] disagrees with our value, the Q_{EC} value with the 124 keV γ-ray gate in a Ge detector (Q_{EC} = 5704(128) keV [19]) yields a mass excess of −65824(129) keV in agreement with our value. As a summary, the differences in the mass excesses may be explained by the uncertainties in the determination of β^+ end-point energies.

4.2.3 ^{82}Y

The isomer at 402.63 keV (268 ns) in ^{82}Y was too short-lived for JYFLTRAP and was not observed. The measured mass excess for the ground state, −68060(6) keV, disagrees slightly with the AME value, −68190(100) keV. In ref. [18], a 574 keV γ transition in ^{82}Sr was used to gate the β^+ spectrum and the measured Q_{EC} value was 7868(185) keV. The calculated mass excess of −68140(186) keV agrees with our value. However, the Q_{EC} value of 7793(123) keV [19] with a mass excess of −68215(124) keV disagrees slightly with our value. Similar to ^{81}Y, the γ transition gate in the Ge detector gives a higher Q_{EC} value of 7820(162) keV [19] and a mass excess of −68188(163) keV in agreement with our value.

4.2.4 ^{83}Y

The measured mass excess of ^{83}Y, −72170(6) keV, deviates from the AME value, −72330(40) keV. ^{83}Y has an isomeric state at 61.98 keV (2.85 min) which could not be resolved in the JYFLTRAP. The Q_{EC} value of 4571(85) keV for the isomeric beta decay was derived from the β^+ spectrum gated by a 422 keV transition in ^{83}Sr in [18]. It yielded a mass excess of −72286(86) keV for the ground state. Q_{EC} values of 4260(80) keV [25] and 4411(50) keV [19] based on β^+ spectra in coincidence with a 36 keV γ transition in ^{83}Sr correspond to the ground-state mass excesses of −72535(81) keV and −72384(51) keV, respectively. In ref. [19], a Q_{EC} value of 4644(84) keV for the isomeric beta decay was also measured. The mass excesses for the isomeric state, −72224(86) keV [18] and −72151(85) keV [19], agree with the measured JYFLTRAP value but the ground-state values from all beta-decay experiments deviate from it. On the other hand, the errors in the end-point energies are so large that it cannot be concluded that we had measured the isomeric state. In fact, the ground state ($9/2^+$) should be more populated in heavy-ion fusion-evaporation reactions than the isomeric state ($3/2^-$) which suggests that we have measured the ground-state mass.

4.3 Zr isotopes

The measured Zr masses are shown in fig. 7 and discussed below.

4.3.1 ^{83}Zr

The isomeric state at 52.72 keV (530 ns) in ^{83}Zr is too short-lived to be observed at JYFLTRAP. The measured ground-state mass excess of −65908(7) keV was 552 keV higher than the AME value of −66460(100) keV. The AME value is based on the end-point of a β^+ spectrum in coincidence with 56 keV, 255 keV, 304 keV and 360 keV γ transitions in ^{83}Y [19]. The resulting Q_{EC} value for the beta decay to the ^{83}Y^m (2.85 min) state was 5806(85) keV which converts to a mass excess of −66464(94) keV when the AME value for ^{83}Y^m is applied. The Q_{EC} value of [19] was already commented to be too low in [26]. Namely, in ref. [26] the end-point energy of the beta-delayed proton spectrum from ^{83}Zr was determined. The measured $Q_{EC} - B_p$ was 2750(100) keV corresponding to a mass excess of −65970(115) keV, where the proton binding energy and the mass excess of ^{83}Y have been taken from the AME tables. With the mass of ^{83}Y measured in this work, this results in a mass excess of −65810(108) keV, still in agreement with our value.

The $Q_{EC} - B_p$ value calculated from the Q_{EC} value of [19] is only 2196(90) keV which is clearly too low for the beta-delayed proton spectrum presented in [26]. Probable isomerism and complex decays of the nuclides were suggested to explain this discrepancy in [26]. Further support for the work by Hagberg *et al.* [26] comes from this experiment. The mass excess measured at JYFLTRAP agrees with [26] and not with [19]. In addition, the Q_{EC} value determined from the mass excesses of ^{83}Y and ^{83}Zr in this experiment is 6263(9) keV which is much higher than Q_{EC} = 5868(85) keV from ref. [19].

4.3.2 ^{84}Zr

The mass of ^{84}Zr was measured for the first time. The obtained mass excess agrees well with the AME value based on the systematics. As ^{84}Zr is situated in the rp process region, its mass is useful, *e.g.*, for the estimation of proton capture reaction rates on ^{83}Y and ^{84}Zr. The beta-decay

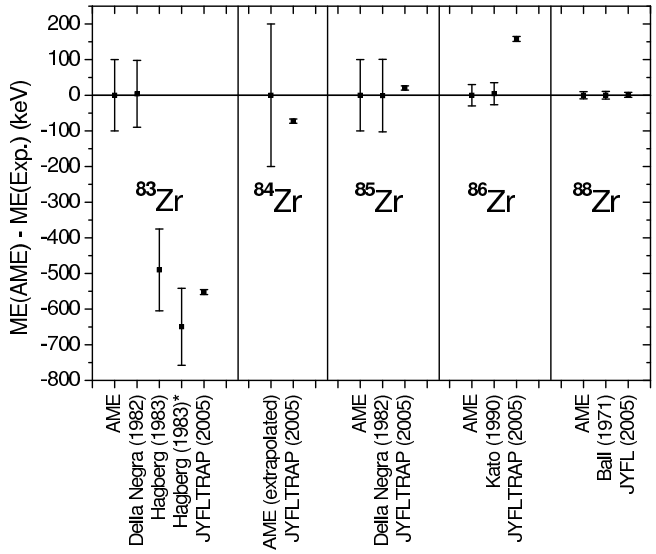

Fig. 7. Mass excesses of the measured Zr isotopes relative to AME values [14]. The error bars represent only the uncertainties of the corresponding experiments. The labels refer to beta-decay experiments of Della Negra *et al.* [19] and Hagberg *et al.* [26] and to reaction studies done by Kato *et al.* [27] and Ball *et al.* [28]. The ^{83}Zr value marked with an asterisk has been calculated with the mass excess of the daughter nucleus ^{83}Y measured in this experiment at the JYFLTRAP. The other mass excesses have been calculated with the respective AME values.

Q_{EC} value for ^{84}Zr can now be calculated from the AME mass excess of ^{84}Y, $Q_{EC} = 2740(90)$ keV. The proton separation energy for ^{84}Zr can be determined as well from the experimental masses of ^{83}Y and ^{84}Zr for the first time, $S_p = 6536(9)$ keV.

4.3.3 ^{85}Zr

The AME value for the mass excess of ^{85}Zr is $-73150(100)$ keV. It is based on the end-point of the β^+ spectrum in coincidence with 416 keV and 453 keV γ transitions in ^{85}Y [19]. The mass excess obtained at JYFLTRAP, $-73170(6)$ keV, agrees nicely with the AME value. The measured mass corresponds to the ground state as it is about 40 times more produced at HIGISOL than the isomeric state at 292.2 keV [6] and no second resonance was observed when scanning a wider frequency range.

4.3.4 ^{86}Zr

The measured mass excess of ^{86}Zr, $-77958(7)$ keV, differs significantly from the AME value, $-77800(30)$ keV. The AME value is based on a Q value of $-40136(30)$ keV for the reaction ^{90}Zr(α, ^{8}He)^{86}Zr [27]. The difference can be explained with low statistics in the momentum (position) spectrum in [27]. Namely, there were only 7 counts in 80 channels (with a maximum of 2 counts/10 channels) in the momentum spectrum. A peak centroid with an accuracy of ± 8.1 channels (± 26 keV) was fitted on this spectrum. The estimated total error of the reaction Q value was given as 30 keV which took into account the errors caused by the uncertainties in the incident energy (± 14 keV), in the target thickness (± 5 keV) and in the masses of ^{90}Zr (± 2 keV) and α-particle (less than 1 keV) [27]. A more realistic error estimation with an error for the peak centroid of about ± 40 channels summed with the systematic errors would give roughly an error of ± 150 keV for the reaction Q value which would be in agreement with the JYFLTRAP value.

4.3.5 ^{88}Zr

The measured mass excess of $-83624(7)$ keV agrees very well with the AME value: the difference is only 1 keV. The AME value is based on a Q value of $-12805(10)$ keV for the reaction ^{90}Zr(p, t)^{88}Zr [28].

4.4 Nb isotopes

Figure 8 shows the measured Nb isotopes together with the AME values and previous mass measurements. The large deviations from the AME mass excesses in ^{85}Nb and ^{86}Nb might be explained if the masses of isomeric states instead of ground states had been measured, as discussed in sect. 4.1. Only the mass of ^{88}Nb agrees with the AME value. The mass measurements of ^{85,86,88}Zr make it possible to determine Q_{EC} values for ^{85,86,88}Nb. With the mass of ^{84}Zr, a proton separation energy for ^{85}Nb can be experimentally determined for the first time. The measured Zr masses have been taken into account in the derivation of the Nb mass excesses from beta-decay experiments for these nuclides.

4.4.1 ^{85}Nb

The measured mass excess, $-66273(7)$ keV, is 877 keV higher than the AME value, $-67150(220)$ keV. The AME value is based on the end-point of a β^+ spectrum in coincidence with a 50 keV γ transition in ^{85}Zr [29]. The Q_{EC} value of 6100(200) keV [29] yields a mass excess of $-67050(224)$ keV with the AME value for ^{85}Zr and a mass excess of $-67070(224)$ keV with the mass excess of ^{85}Zr measured in this work, still about 800 keV off from our value.

The AME value for the mass excess of ^{85}Nb is based on the Q_{EC} value given incorrectly as $Q_{EC} = 6000(200)$ keV in the abstract of [29]. The Q_{EC} value determined from the mass excesses of ^{85}Nb and ^{85}Zr measured in this experiment is 6898(9) keV, about 900 keV from the adopted AME value. Also the proton separation energy determined from the measured masses of ^{84}Zr and ^{85}Nb, $S_p = 2144(9)$ keV differed about 800 keV from the adopted AME value.

The differences in mass excesses and Q_{EC} values can have several sources. Firstly, the energy calibration of the beta detector in [29] was done with the Q_{EC} values of

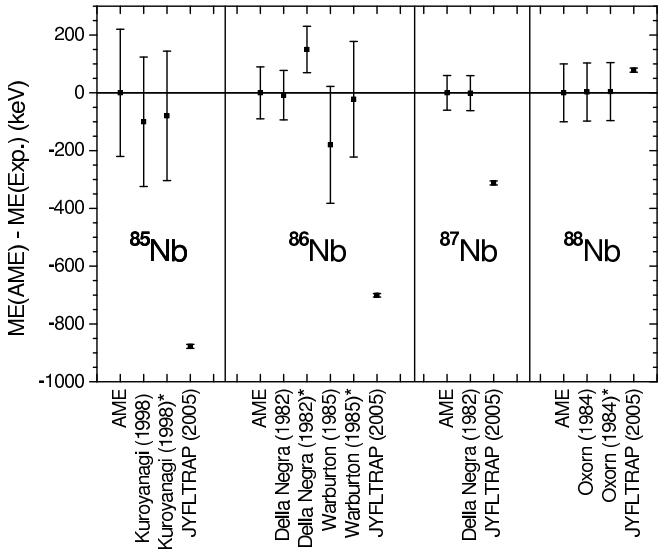

Fig. 8. Mass excesses of the measured Nb isotopes relative to AME values [14]. The error bars represent only the uncertainties of the corresponding experiments. The labels refer to beta-decay experiments of Kuroyanagi *et al.* [29], Della Negra *et al.* [33], Warburton *et al.* [34] and Oxorn and Mark [37]. The values of ^{85,86,88}Nb marked with an asterisk have been calculated with the mass excesses of the corresponding daughter nuclei ^{85,86,88}Zr measured in this experiment at the JYFLTRAP. The other mass excesses have been calculated with AME values for daughter nuclides.

^{83}Y (4.411 MeV), ^{83}Zr (5.806 MeV) and ^{82}Y (7.793 MeV) which were found to be about 214 keV, 395 keV and 155 keV too low in this experiment.

Another explanation for the discrepancy in the masses could be that the beta decay of ^{85}Nb feeds mainly higher-lying levels which then decay to the first excited state at 50 keV in ^{85}Zr. The high-spin studies of ^{85}Zr have revealed a $11/2^+$ state at 854 keV and a $13/2^+$ state at 872 keV [30, 31]. These states decay to the state at 50 keV by 804 keV and 822 keV γ transitions, respectively.

The third possibility is that the mass excess measured in this work is for an isomeric state in ^{85}Nb instead of the ground state. In a spectroscopic experiment [32], a 759 keV γ transition with a half-life of 12(5) s was observed at mass $A = 85$ and it was suggested to originate either from a β-decaying isomer in ^{85}Nb or in ^{85}Mo. In addition, a 69 keV transition with a half-life of 3.3(9) s was observed at mass $A = 85$ in [6]. This transition belongs most likely to an isomeric state in ^{85}Nb. The origin of the 69 keV transition from the β^+ decay of ^{85}Mo was unlikely as there was no coincidence with the annihilation radiation. As a summary, the energy of the isomeric state in ^{85}Nb is uncertain. The energy range covered in the JYFLTRAP was about $\pm$900 keV from the resonance and no indication of an isomer was found. Therefore, the isomeric state suggested by the systematics of odd-A Nb isotopes (see ref. [6]) should lie above 900 keV, its half-life is below 500 ms or it is much less produced than the ground state. In ref. [6], the production ratio of the isomeric state to the ground state was roughly 1 : 2 which supports the last option. Most likely the isomeric state was not produced enough for the observation in the trap.

4.4.2 ^{86}Nb

The measured mass excess of ^{86}Nb, $-69129(6)$ keV, differs -701 keV from the AME value of $-69830(90)$ keV. The AME value is based on [33] which measured the end-point of a β^+ spectrum in coincidence with 752 keV, 914 keV and 1003 keV γ transitions in ^{86}Zr. The adopted Q_{EC} value was 7978(80) keV which converts to a mass excess of $-69822(86)$ keV with the AME mass excess for ^{86}Zr. With the JYFLTRAP mass excess of ^{86}Zr, the resulting mass excess is $-69980(81)$ keV which is still far away from the measured mass excess of ^{86}Nb. The Q_{EC} value determined from the mass excesses of ^{86}Zr and ^{86}Nb measured in this work is 8829(9) keV.

The Q_{EC} value of [33] was claimed to be wrong already in ref. [34]. Namely, an erroneous 100% beta feeding was assumed to the 2670 keV level in ^{86}Zr in [33]. In ref. [34] almost equally strong beta feedings to states at 3254 keV and 3418 keV were observed and the Q_{EC} value was calculated from the weighted average for the final ^{86}Zr states. By using 752 keV, 916 keV and 1003 keV γ transition gates for the β^+ spectrum, a Q_{EC} value of 8150(200) keV was concluded in [34]. The deduced mass excesses of ^{86}Nb, $-69650(203)$ keV (from the AME mass excess of ^{86}Zr) and $-69808(201)$ keV (from the mass excess of ^{86}Zr measured in this work), are still too low compared to our value. Thus, the discrepancy cannot solely be explained by the neglected beta-decay feedings to higher states than 2670 keV unless possible beta-decay feedings to even higher states of ^{86}Zr have been missed in [34].

An isomer with a half-life of 56 s in ^{86}Nb was suggested in ref. [35] based on the time behavior of Zr KX-rays in coincidence with the sum of the 752 keV, 915 keV and 1003 keV γ transitions in ^{86}Zr. This isomeric state with an unknown energy was not confirmed in [6]. In ref. [36], the existence of this isomer was considered as uncertain as the result has not been confirmed in later experiments. It is also surprising that the ground-state assignment of ^{86}Nb is not experimentally verified, and thus, the lowest observed state with a half-life of 88 s (6^+) is considered as an isomer at an energy of $0 + X$ keV [36]. In this experiment, we could not find an isomeric state within 450 keV from the resonance in the JYFLTRAP. This means that the suggested isomer is located above 450 keV or is much less produced than the ground state.

4.4.3 ^{87}Nb

The measured mass excess of ^{87}Nb, $-73868(7)$ keV, differs significantly from the AME value, $-74180(60)$ keV. This discrepancy cannot be explained by the known isomeric state as it is located at 4 keV which falls within the error bars of the determined resonance. The AME mass excess is based on the end-point of a β^+ spectrum in coincidence

with 201 keV and 617 keV γ transitions of ^{87}Zr [33]. The Q_{EC} value of 5169(60) keV [33] is 311 keV lower than the Q_{EC} determined from the masses of ^{87}Zr [14] and ^{87}Nb from this work, $Q_{EC} = 5480(11)$ keV. Either the energy calibration of the β^+ detector in [33] is off or the beta decay of ^{87}Nb to higher-lying states has been underestimated. Note that the mass excess of ^{86}Nb derived from [33] was also too low compared to this work.

4.4.4 ^{88}Nb

The measured mass excess of ^{88}Nb agrees with the AME value. The AME mass excess is based on a measurement of the end-point of a β^+ spectrum in coincidence with a 503 keV transition in ^{88}Zr [37]. The Q_{EC} value of 7550(100) keV [37] is in agreement with the value based on ^{88}Zr and ^{88}Nb masses measured in this work, $Q_{EC} =$ 7476(9) keV. The isomer suggested to lie at 40(140) keV (7.8 min) was not observed within 310 keV from the resonance. Either the production rate of the isomer was too low or its energy is so close to the ground state that it could not be resolved.

Table 4. Q_{EC} values for the measured nuclides. The mass of the daughter nucleus is from this experiment for ^{83}Zr, ^{85}Nb, ^{86}Nb and ^{88}Nb (marked with †). For the others, the mass of the daughter nucleus is from ref. [14]. The last column lists the difference between the determined Q_{EC} value and the adopted AME value [14].

Nuclide	Q_{EC}(keV)		Difference (keV)
	This work	AME [14]	
^{80}Y	9164(10)	9090(180)	74(180)
^{81}Y	5819(9)	5510(60)	309(60)
^{82}Y	7948(9)	7820(100)	128(100)
^{83}Y	4625(12)	4470(40)	155(50)
^{83}Zr	6263(9)†	5870(90)	393(90)
^{84}Zr	2740(90)	2670(220)#	70(240)
^{85}Zr	4670(20)	4690(100)	−20(110)
^{86}Zr	1326(16)	1480(30)	−154(40)
^{88}Zr	675(7)	676(10)	−1(12)
^{85}Nb	6898(9)†	6000(200)	898(200)
^{86}Nb	8829(9)†	7980(80)	849(80)
^{87}Nb	5480(11)	5170(60)	310(60)
^{88}Nb	7476(9)†	7550(100)	−74(100)

5 Conclusions

With the measured absolute masses, the accuracies of proton separation energies and Q_{EC} values for 12 neutron-deficient nuclides have been improved substantially (see tables 3, 4 and fig. 9). The Q_{EC} value for ^{84}Zr and proton separation energies for ^{84}Zr and ^{85}Nb have been determined experimentally for the first time.

Almost all of the studied nuclides lie on the path of the rp process and are involved in the proton captures (see fig. 1). The masses of these nuclides have been measured with uncertainties of less than 10 keV required for detailed rp process calculations [4]. Large deviations (several hundreds of keV) to the adopted AME values have been found except for ^{80}Y, ^{84,85,88}Zr and ^{88}Nb which all agree with the AME values. Many of the AME mass excesses based on beta-decay experiments differ significantly from

Table 3. Proton separation energies for the measured nuclides. The mass of the $(Z-1, N)$ nucleus is from this experiment for ^{83}Zr, ^{84}Zr, ^{85}Nb, ^{86}Nb and ^{87}Nb (marked with †). For the others, the AME mass of the $(Z-1, N)$ nucleus is used [14]. Proton separation energies for ^{84}Zr and ^{85}Nb have been experimentally determined for the first time. The last column lists the difference between the determined S_p value and the corresponding AME value [14].

Nuclide	S_p(keV)		Difference (keV)
	This work	AME [14]	
^{80}Y	2956(11)	3030(180)	−74(180)
^{81}Y	2690(9)	3000(60)	−310(60)
^{82}Y	3821(9)	3950(100)	−129(100)
^{83}Y	3451(9)	3610(40)	−159(40)
^{83}Zr	5137(9)†	5560(140)	−423(140)
^{84}Zr	6536(9)†	6460(200)#	76(200)
^{85}Zr	6300(90)	6280(140)	20(170)
^{86}Zr	7410(20)	7250(40)	160(50)
^{88}Zr	7895(7)	7893(10)	2(12)
^{85}Nb	2144(9)†	2950(300)#	−806(300)
^{86}Nb	3248(9)†	3970(130)	−722(130)
^{87}Nb	3199(9)†	3670(70)	−471(70)
^{88}Nb	4090(11)	4010(100)	80(100)

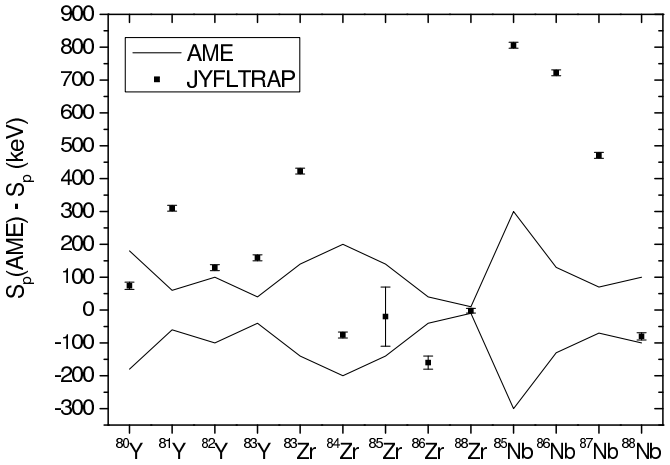

Fig. 9. Proton separation energies for the measured nuclides relative to AME values. The two lines show the corridor of uncertainties taken from ref. [14]. The mass of the $(Z-1, N)$ nucleus is from this experiment for ^{83}Zr, ^{84}Zr, ^{85}Nb, ^{86}Nb and ^{87}Nb. For the others, the AME mass [14] of the $(Z-1, N)$ nucleus has been used.

the directly measured values for these neutron-deficient nuclides. A similar tendency has also been observed for neutron-rich nuclides in direct mass measurements at ESR [38] and at JYFLTRAP [39]. In the studied cases it is obvious (see fig. 9), especially for Nb isotopes, that the estimates for the proton separation energies of lightest isotopes will have to be revised significantly which could even impact the estimated position of the proton drip line. These data will provide important contribution to more reliable predictions of binding energies at main rp process nuclei.

This work has been supported by the EU 6th Framework program "Integrating Infrastructure Initiative - Transnational Access", Contract Number: 506065 (EURONS) and by the Academy of Finland under the Finnish Center of Excellence Program 2000-2005 (Project No. 44875, Nuclear and Condensed Matter Physics Program at JYFL). The support via the Finnish-Russian interacademy agreement (Project No. 8) is gratefully acknowledged. The authors thank H. Schatz for his valuable comments on the manuscript of this article.

References

1. R.K. Wallace, S.E. Woosley, Astrophys. J. Suppl. **45**, 389 (1981).
2. H. Schatz *et al.*, Phys. Rep. **294**, 167 (1998).
3. H. Schatz *et al.*, Phys. Rev. Lett. **86**, 3471 (2001).
4. H. Schatz, K.E. Rehm, to be published in Nucl. Phys. A.
5. Yu.N. Novikov *et al.*, Eur. Phys. J. A **11**, 257 (2001).
6. A. Kankainen *et al.*, Eur. Phys. J. A **25**, 355 (2005).
7. P. Dendooven *et al.*, Nucl. Instrum. Methods Phys. Res. A **408**, 530 (1998).
8. J. Äystö, Nucl. Phys. A **693**, 477 (2001).
9. A. Nieminen *et al.*, Nucl. Instrum. Methods Phys. Res. A **469**, 244 (2001).
10. V.S. Kolhinen *et al.*, Nucl. Instrum. Methods Phys. Res. A **528**, 776 (2004).
11. M. König *et al.*, Int. J. Mass Spectrom. Ion. Proc. **142**, 95 (1995).
12. S. Rinta-Antila *et al.*, Phys. Rev. C **70**, 011301 (2004).
13. K. Blaum *et al.*, J. Phys. B: At. Mol. Opt. Phys. **36**, 921 (2003).
14. G. Audi, A.H. Wapstra, C. Thibault, Nucl. Phys. A **729**, 337 (2003).
15. A.H. Wapstra, G. Audi, C. Thibault, Nucl. Phys. A **729**, 129 (2003).
16. G. Audi *et al.*, Nucl. Phys. A **729**, 3 (2003).
17. J. Huikari *et al.*, Nucl. Instrum. Methods Phys. Res. B **222**, 632 (2004).
18. C.J. Lister *et al.*, Phys. Rev. C **24**, 260 (1981).
19. S. Della Negra *et al.*, Z. Phys. A **307**, 305 (1982).
20. M. Shibata *et al.*, J. Phys. Soc. Jpn. **65**, 3172 (1996).
21. S. Issmer *et al.*, Eur. Phys. J. A **2**, 173 (1998).
22. C.J. Barton *et al.*, Phys. Rev. C **67**, 034310 (2003).
23. A.S. Lalleman *et al.*, Hyperfine Interact. **132**, 315 (2001).
24. M. Chartier *et al.*, J. Phys. G **31**, S1771 (2005).
25. C. Deprun *et al.*, Z. Phys. A **295**, 103 (1980).
26. E. Hagberg *et al.*, Nucl. Phys. A **395**, 152 (1983).
27. S. Kato *et al.*, Phys. Rev. C **41**, 1276 (1990).
28. J.B. Ball, R.L. Auble, P.G. Roos, Phys. Rev. C **4**, 196 (1971).
29. T. Kuroyanagi *et al.*, Nucl. Phys. A **484**, 264 (1988).
30. A. Jungclaus *et al.*, Z. Phys. A **352**, 3 (1995).
31. S.K. Tandel *et al.*, Phys. Rev. C **65**, 054307 (2002).
32. M. Oinonen *et al.*, Nucl. Instrum. Methods Phys. Res. A **416**, 485 (1998).
33. S. Della Negra, D. Jacquet, Y. Le Beyec, Z. Phys. A **308**, 243 (1982).
34. E.K. Warburton *et al.*, Phys. Rev. C **31**, 1211 (1985).
35. T. Shizuma *et al.*, Z. Phys. A **348**, 25 (1994).
36. B. Singh, Nucl. Data Sheets **94**, 1 (2001).
37. K. Oxorn, S.K. Mark, Z. Phys. A **316**, 97 (1984).
38. M. Matos *et al.*, *Proceedings of the EXON-04 Conference, Peterhof, July 2005* (World Scientific, Singapore, 2005) p. 90.
39. U. Hager *et al.*, Phys. Rev. Lett. **96**, 042504 (2006).